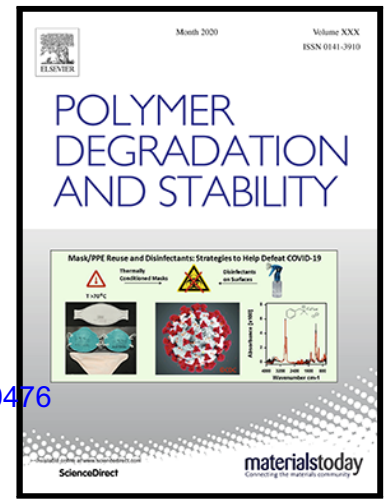

Insights into the effect of different macromolecular architectures on the charring ability of polyethylene

A. Frache , R. Arrigo , G. Malucelli , G. Camino

PII: S0141-3910(23)00226-4
DOI: https://doi.org/10.1016/j.polymdegradstab.2023.110476
Reference: PDST 110476

To appear in: *Polymer Degradation and Stability*

Received date: 30 May 2023
Revised date: 11 July 2023
Accepted date: 13 July 2023

Please cite this article as: A. Frache , R. Arrigo , G. Malucelli , G. Camino , Insights into the effect of different macromolecular architectures on the charring ability of polyethylene, *Polymer Degradation and Stability* (2023), doi: https://doi.org/10.1016/j.polymdegradstab.2023.110476

Highlights

- the isothermal TGA behaviour of different PEs gives dissimilar residue and stability
- hydroperoxidation and dehydrogenation reactions compete during PE thermo-oxidation
- Macromolecular architecture of polyethylenes affects its charring ability

Insights into the effect of different macromolecular architectures on the charring ability of polyethylene

A. Frache [1,2*], R. Arrigo [1,2], G. Malucelli [1,2], G. Camino [1]

[1] *Department of Applied Science and Technology, Politecnico di Torino, viale Teresa Michel 5, Alessandria, Italy*

[2] *Local INSTM unit*

Abstract

The induction period preceding the ignition is a fundamental stage in controlling the protection of polymeric materials from fire. In fact, at this stage, the formation of a non-pyrolyzable carbonaceous layer (char) onto the material surface could prevent the development of a sustained flame, hence delaying or preventing polymer burning. In this work, the charring ability of four samples of high- and low-density polyethylene was evaluated in different scenarios, namely isothermal oxidative conditions and cone calorimetry tests at different heat fluxes, aiming at assessing the possible influence of the polymer macromolecular architecture on their charring ability. First, the selected polymers were characterized from a thermal and rheological point of view; the obtained results allowed for disclosing the different microstructure of the materials, in terms of molecular weight and possible presence of short- or long-chain branching. Then, isothermal thermogravimetric analyses and cone calorimetry tests were performed, demonstrating a different charring ability of the investigated polyethylenes. Finally, the observed behaviours were correlated to the different chemical structure and to the specific macromolecular architecture of the polymers, allowing a systematic evaluation of the relationship between the molecular weight or the presence of branched structures and the mechanism and rate of char formation.

Keywords: fire behaviour; polyethylene; ignition behaviour; charring; macromolecular architecture.

1. Introduction

Organic polymers ignite following a very complex mechanism, which involves the occurrence of several physical and chemical events [1-2]. Briefly, the ignition of polymers occurs when the concentration of fuel in the gas phase (the former being produced through reactions of chain fragmentation leading to the evolution of volatile compounds) reaches the lower flammability limit [3-4]. In these conditions, it is possible obtaining a sustained flame resulting from an external ignition or by self-ignition when the gas phase is above the self-ignition temperature [5]. Actually,

the reactions of thermal decomposition of the polymer macromolecules forming volatiles are in competition, at this stage, with oxidative dehydrogenation reactions. In particular, it is known that oxygen can interact with the polymer chains, inducing the formation of secondary carbon radicals that are prone to recombine by crosslinking or polycyclic structures further evolving with the formation of carbonaceous residues on the polymer surface [6]. It has been demonstrated that for most thermoplastics, and in particular for polyolefins, the first phenomenon often overwhelms the charring mechanism [7-8]. Therefore, for non-charring polymers, the thermally induced decomposition of the macromolecules continuously releases heat, which irradiates onto the unburned material, thus continuing pushing pyrolysis and combustion until the fire extinguishment due to the lack of heat, fuel or oxygen [9].

From a general point of view, the typical involvement of polymers in fires occurs through their chemical degradation taking place in three steps: ignition, combustion, and smouldering. In these steps, the polymer is exposed to different physico-chemical degradation conditions: thermal oxidative in ignition and smouldering, and anaerobic pyrolysis in combustion [10-11]. Having in mind the fire scenario, it appears that the most profitable approach to protect polymers from fire should primarily address the ignition stage when the rate of their chemical degradation processes, producing flammable volatiles, is quite low owing to the relatively low temperature to which they are exposed. Nevertheless, the research that started in the 70's of the last century, aiming at developing methods to make polymers slow-burning materials (fire/flame retardant polymers), has almost exclusively addressed the polymer combustion step. This is essentially due to the fact that a bench scale testing apparatus, scientifically reproducing polymer burning (Oxygen Consumption Calorimeter or Cone Calorimeter) including the evaluation of the ignition step, has only become available in the 80's of the last century [12]. The universal diffusion of the cone calorimeter in the fire retardant research groups makes it today worth extending fire retardancy studies to the delay or suppression of polymers ignition.

The access to the study of the polymer materials behaviour in the ignition step supplies the thermal oxidation mechanism of the polymer, which produces the volatile products that ignite, hence starting the combustion process. This information is particularly useful in the case of the quite common fire scenario, in which the polymer material is at the origin of the fire by exposure to a low-energy heat source for a relatively long time before ignition conditions are reached. In fact, in these cases, a polymer fire protection strategy based on hindering polymer degradation could be sought, leading to ignition delay beyond rescue time or possibly ignition suppression.

While the combustion of a polymer material exposed to a developed fire has been shown to be properly simulated by the polymer exposed to the radiant heater of the cone calorimeter operated at

an irradiation of the order of 50 kW/m^2 [13] the simulation of the ignition by a low energy heat source comparable to that of a cigarette (5W) or a burning candle (80W) [14] requires much lower irradiation that could be tentatively set around 20 kW/m^2 or even below.

The ignition process is bound to be kinetically controlled because it involves a heterophasic reaction between oxygen of air and the solid or liquid polymer material [2]. The degree of kinetic control and therefore the dependence of ignition on irradiation is related to the polymer chemical reactivity with oxygen and oxygen diffusion rate into the polymer phase. The low irradiance of the cone calorimeter tests provides the time-resolved conditions for collecting all the physical and chemical parameters characterising the ignition process of polymers, including its dependence on exposure irradiance and hence polymer heating rate.

In this work, the charring ability of polyethylenes (PEs) having different macromolecular architectures, in terms of molecular weight and presence of short- or long-branching structures, is thoroughly investigated. It is well-known and extensively described in the literature that PE is able to form char in oxidative conditions at temperatures below the ignition temperature [15-16]. Nevertheless, to the best of the authors' knowledge, the influence of the macromolecular microstructure on the charring ability of this polymer has not systematically been investigated yet. To this aim, the char formation (either in isothermal conditions or during cone calorimetry tests carried out at different heat fluxes) of four samples of high-density and low-density polyethylene, differing for the molecular weight and the presence of short- or long-chain branching points, was studied. The obtained results were then discussed considering the influence of either the different chemical structure or the dissimilar macromolecular architecture of the selected materials on the mechanism of char formation. The disclosed microstructure/charring ability relationships could be very useful to gain fundamental insights into the intrinsic charring characteristics of PE, aiming at better controlling this fundamental stage of its fire behaviour and selecting the more appropriate flame-retardant strategy.

2. Materials and methods

2.1 Materials

Different grades of polyethylene were used. Table 1 reports the commercial names, the values of melt flow index (MFI) and density provided by the suppliers. Furthermore, Table 1 lists the codes used hereinafter to indicate the different materials; each sample was coded as high viscosity (HV) or low viscosity (LV), according to the value of its MFI. All the materials were used without any further purification.

Table 1: Commercial names, suppliers, code and main properties of PEs samples.

Material	Supplier	Code	MFI [190 °C/2.16 kg] (g/10min)	Density (g/cm^3)
Eraclene MP90U	Versalis	HDPE_LV	7	0.960
Lupolen 5021DX	LyondellBasell	HDPE_HV	0,25	0.950
Alcudia PE022	Repsol	LDPE_LV	70	0.915
Lupolen 2420F	LyondellBasell	LDPE_HV	0,75	0.923

2.2 Characterization Techniques

Differential Scanning Calorimetry (DSC) characterization was performed using a Q20 apparatus (TA Instrument, New Castle, DE, USA), on samples of about 8 mg placed in closed aluminium pans. The following thermal cycle was applied: (*i*) a first heating ramp from 25 to 200 °C, (*ii*) a cooling ramp from 200 to 25 °C and (*iii*) a second heating step up to 200 °C. A heating or cooling rate of 10 °C/min was selected. The crystallization temperature (Tc), crystallization enthalpy (ΔH_c), melting temperature (T_m), and melting enthalpy (ΔH_m) were evaluated, using the thermograms recorded during the cooling and the 2nd heating ramp. The crystallinity degree (X_c) was calculated using the following formula (Equation (1)):

$$Xc = \frac{\Delta H_m}{\Delta H_{100}} * 100 \quad (1)$$

where ΔH_{100} represents the melting enthalpy of the 100% crystalline polymer (293 J/g [17]).

Rheological analyses were carried out using a parallel plate-plate ARES (TA Instrument, New Castle, DE, USA) strain-controlled rheometer (plate diameter: 25 mm; gap between the plates: 1 mm). Frequency sweep tests were performed to evaluate the complex viscosity as a function of frequency. The tests were carried out in a frequency range between 10^{-1} and 10^{2} rad/s, at a temperature of 190 °C, and selecting a strain amplitude of 10% (within the linear viscoelastic range for all investigated materials, as assessed by preliminary strain sweep measurements). The obtained experimental data were fitted using the Cross model (Equation 2):

$$\eta(\omega) = \frac{\eta_0}{1 + [(\lambda\omega)^{1-n}]} \quad (2)$$

where η_0 is the zero-shear viscosity, λ the relaxation time and *n* the flow index. Relaxation spectra were calculated using data coming from small amplitude oscillatory shear measurements, using the method proposed by Honerkamp and Weese [18]. Time sweep tests were carried out at 250 °C, 10 % strain amplitude, and 10 rad/s frequency. Samples for the rheological characterizations were obtained through a compression moulding step in a hot-plates press operating at 190°C and 100 bar.

The thermal and thermo-oxidative behaviour of the investigated polymers was assessed through thermogravimetric analysis (TGA) using a Q500 system (TA Instrument, New Castle, DE, USA); the samples were heated from 50 to 800 °C at 10 °C/min, under both nitrogen and air flow (35 and 25 mL/min, respectively). The tests were performed placing about 10 mg of sample in open alumina pans. $T_{2\%}$ (the temperature, at which 2% weight loss occurs), T_{max} (the temperature, at which reported. Isothermal analyses were performed by keeping the sample at 320 °C in air for 60 min up to constant weight and then heating it up to 650 °C at a heating rate of 10°C/min.

The times to ignition (TTIs) of the polymers were evaluated through cone calorimetry tests according to the ISO 5660 standard, using a Noselab Ats (Nova Milanese, Italy) instrument. Square samples (50 × 50 × 3 mm^3, obtained through compression moulding with a hot plate press operating at 190°C and 100 bar) were exposed to 20 and 35 kW/m^2 heat fluxes in horizontal configuration. The specimens were wrapped in aluminium foil except for the upper face, maintaining a distance of 25 mm between the sample surface and the cone heater. The temperatures involved before combustion were recorded using a K-type, Inconel 600 sheathed and MgO insulated, thermocouples by Tersid (I), compliant with ASTM E585, with an outer diameter of 0.5 mm, and wire diameter of 0.1 mm, following an experimental procedure reported in [2]. Briefly, the thermocouples were placed and supported to maintain the contact with the upper surface of the specimen during the whole experiment. In particular, the position of the thermocouples was properly selected to allow small vertical displacement of its tip, hence providing a good thermal contact with the polymer specimen during the execution of the test. Furthermore, the position of the thermocouples prior to the ignition was carefully checked during each test, invalidating the tests for which the thermocouple lifted off the surface or sank into the molten polymer. Each material was tested at least three times and the results were averaged (experimental error = 5%).

The chemical characterisation of the surfaces of the materials before and after the thermal irradiation was carried out by means of a Frontier FT-IR spectrophotometer (Perkin Elmer, Waltham, MA, USA) equipped with an Attenuated Total Reflection (ATR) diamond probe. ATR-FTIR spectra were recorded in the range from 4000 to 500 cm^{-1}, with 4 cm^{-1} resolution; 16 scans were collected.

3. Results

3.1 Preliminary characterization of PEs

In this section, the results of the preliminary spectroscopic, thermal and rheological characterizations of the investigated PE samples are reported, aiming at gaining some details about their crystallinity content, thermal stability and macromolecular architecture.

3.1.1 ATR-FTIR characterization

Figure 1A shows the ATR-FTIR spectra of the four investigated materials. In the spectra, the typical absorption bands of polyethylene are observable; in particular, the strong intensity bands at 2915 and 2848 cm^{-1} are related to C-H stretching in CH_2 groups, the medium intensity bands at 1472 and 1463 cm^{-1} can be attributed to CH_2 bending deformations and the absorption bands at 728 and 719 cm^{-1} refer to CH_2 rocking vibrations. Furthermore, a small absorption band at 1377 cm^{-1}, associable with the bending of methyl groups, is observed [19].

Figure 1B depicts the enlargement of the spectra in the region, in which the signals associated with CH_2 and CH_3 bending modes appear. The differences noticed in the intensities of the peaks at 1467 and 1377 cm^{-1}, associated with the bending modes of CH_2 and CH_3 groups respectively, can be attributed to the different macromolecular architectures of the four samples of PE. In particular, the calculation of the ratio between the intensities of the peaks related to CH_3 and CH_2 groups can be useful for discriminating between linear or branched topology, as well as for gaining some information about the degree of branching. Concerning the PEs investigated in this study, HDPE_HV and HDPE_LV show a calculated ratio of 0.015 and 0.014, respectively, while values of 0.112 and 0.077 are obtained for LDPE_LV and LDPE_HV samples. On the basis of the obtained values, it is possible inferring that LDPE_LV, which presents the highest ratio, possesses a large amount of short-chain branches (resulting in a great number of -CH_3 terminal groups), while LDPE_HV is characterized by a long-chain branched structure. On the other hand, the different values obtained for the two HDPE samples can be associated with the different lengths (i.e. different molecular weights) of the two linear polymers.

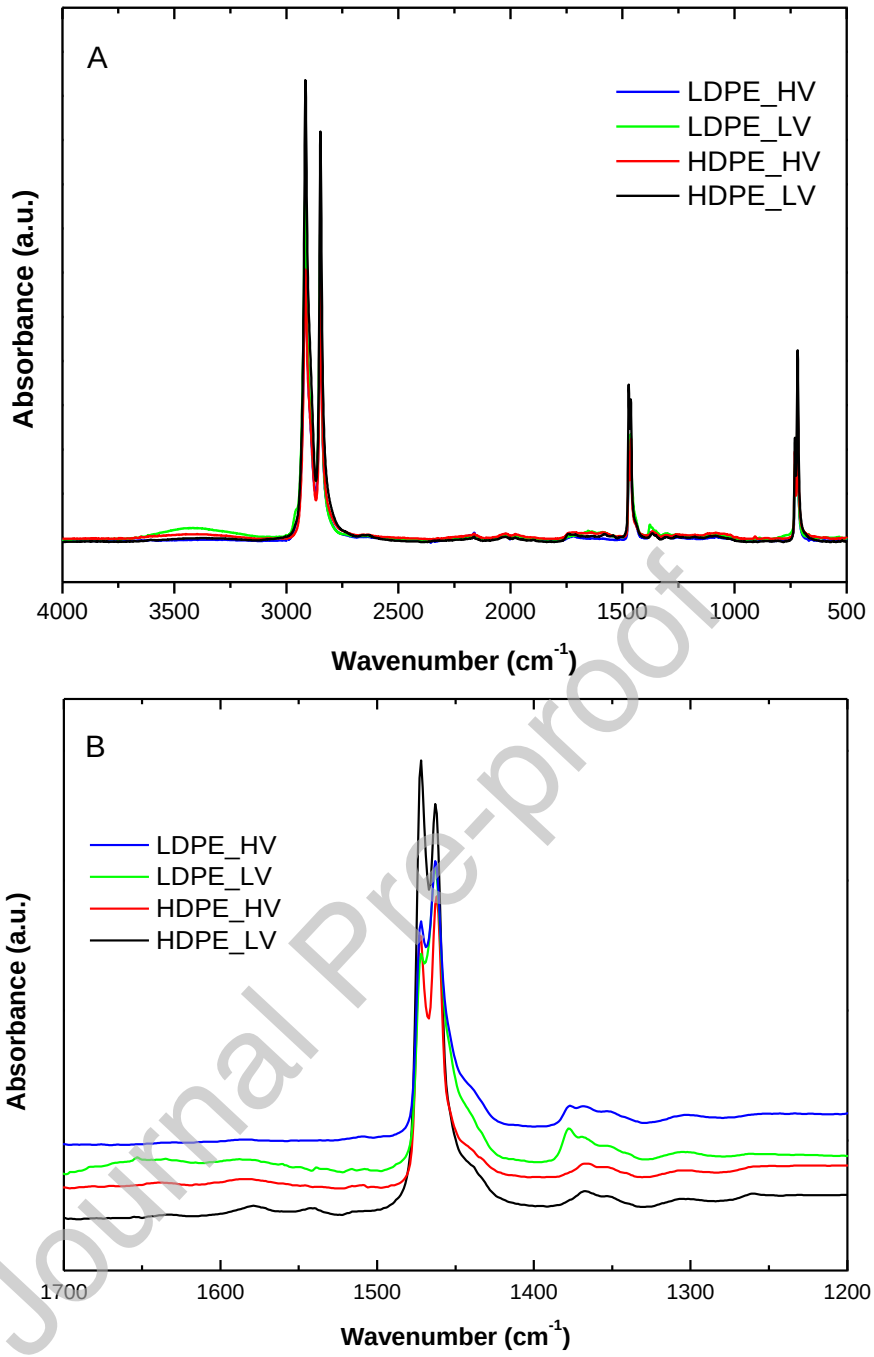

Figure 1. ATR-FTIR spectra for the PEs samples (A) and enlargement of the region between 1700 and 1200 cm^{-1} (B).

3.1.2 DSC characterization

Table 2 collects the main DSC data collected for the different types of polyethylene. Overall, it is worth noting that the LDPE samples present lower values of crystallization and melting temperatures as compared to HDPEs. Furthermore, as expected and well-known, the crystallinity content of the HDPE samples is significantly higher than that of LDPEs [20-21]; in fact, as widely reported in the literature, the prominent linear topology of the HDPE chains promotes the formation

of crystalline structures, while the presence of short- and/or long-chain branching points in LDPEs hinders the polymer crystallization processes [22].

Table 2. Main results from DSC analyses for all investigated materials.

Material	T_c (°C)	T_m (°C)	ΔH_m (J/g)	X_c (%)
HDPE_LV	116.0	135.2	190.7	65.8
HDPE_HV	115.4	131.5	181.7	62.0
LDPE_LV	85.5	103.6	88.0	30.0
LDPE_HV	94.8	114.2	91.2	31.1

3.1.3 Rheological behaviour

Figures 2 (A) and (B) show the complex viscosity curves of the analysed PEs as a function of frequency. Looking at the curves of the two HDPE samples, reported in Figure 2A, HDPE_LV exhibits lower viscosity values as compared to HDPE_HV in the whole investigated frequency range, and a pronounced Newtonian behaviour. This last involves a Newtonian plateau in the low and intermediate frequencies and a mild shear thinning at high frequencies. Conversely, HDPE_HV shows non-Newtonian characteristics, involving a continuous decrease of the complex viscosity over the frequency and a significant shear thinning, typical of highly entangled polymer melts.

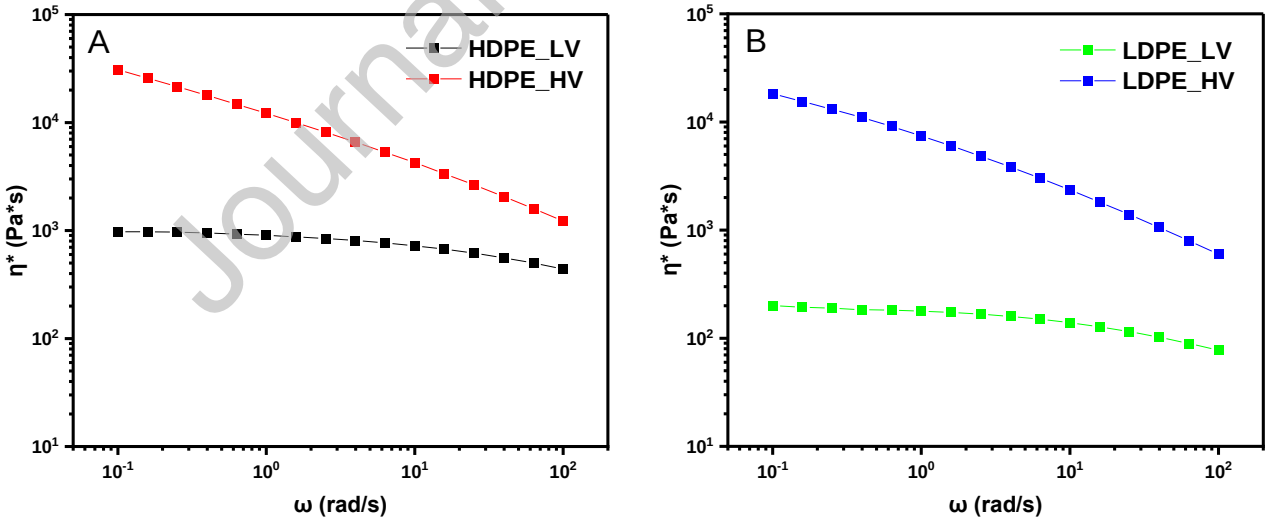

Figure 2: Complex viscosity curves for HDPEs (A) and LDPEs (B) samples.

The differences observed in the behaviour of the two HDPE samples could be associated with a different molecular weight of the two materials, as also suggested by their different MFI values. To confirm this feature, the experimental data were fitted with the Cross model (Equation 2), aiming at

assessing the values of the zero-shear viscosity (η_0), which is a rheological property very sensitive to the polymer molecular weight. The calculated values of η_0, listed in Table 3, confirm what is inferred from the analysis of the complex viscosity curves; therefore, HDPE_HV is characterized by a higher molecular weight than HDPE_LV. As far as the rheological behaviour of LDPEs is concerned (their complex viscosity curves are reported in Figure 2B), LDPE_HV exhibits higher viscosity values than LDPE_LV, and more pronounced non-Newtonian features. The calculated values of η_0 seem to suggest also in this case a different molecular weight for the two materials.

Table 3. Values of zero-shear viscosity for all investigated materials.

Material	**η_0 [Pa s]**
HDPE_LV	$1.02\ 10^3$
HDPE_HV	$7.24\ 10^4$
LDPE_LV	$2.02\ 10^2$
LDPE_HV	$1.82\ 10^4$

Actually, LDPEs have a more complex macromolecular architecture as compared to HDPEs, involving the presence of short- and/or long-chain branching and a great variety of branch topologies. Therefore, the differences observed between the two LDPEs samples could be associated not only with a different molecular weight but also with a different degree or topology of short- and long-chain branching, which cannot be merely ascertained through the assessment of the zero-shear viscosity values. Since the presence of branched structures randomly distributed along the polymer backbone alters the relaxation kinetics of the macromolecular chains by introducing long relaxation modes, a successful method used to detect the level of branching is the analysis of the relaxation spectrum [23]. The comparison between the relaxation spectra of LDPE_HV and LDPE_LV (Figure 3) reveals a very different behaviour for the two samples, which can be associated with dissimilar relaxation mechanisms. In particular, LDPE_LV shows the typical liquid-like behaviour typical of linear or short-chain branched polymers. Conversely, LDPE_HV tends to relax like a pseudo-solid material, with a higher relaxation strength as compared to LDPE_LV; this finding is a clear indication of the introduction of different long-time relaxation modes due to the presence of a high level of long-chain branching [24]. Therefore, the analysis of the rheological behaviour of the two LDPE samples suggests that the macromolecular architecture of LDPE_HV is characterized by a high level of long-chain branching, strongly affecting the material viscosity and its relaxation dynamics. On the other hand, the Newtonian behaviour and the liquid-like features of

LDPE_LV indicate that this material has a lower molecular weight and contains only short-chain branching, resulting in a rheological behaviour similar to those of linear HDPE_LV sample.

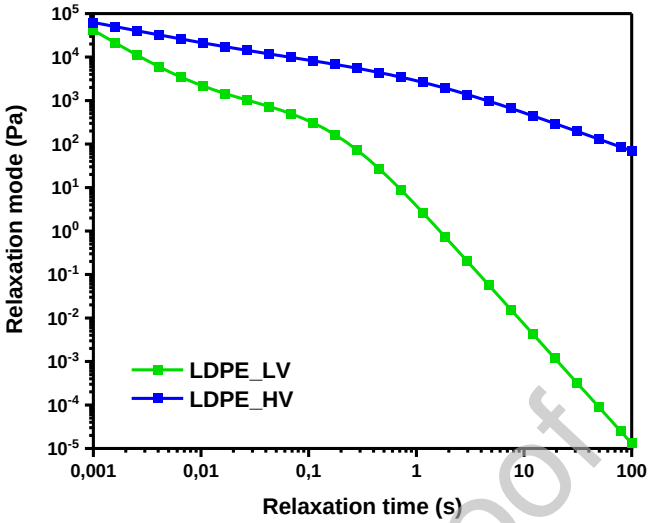

Figure 3. Relaxation spectra of LDPEs samples.

3.1.4 Thermogravimetric analyses

Thermogravimetric analyses were performed in order to evaluate the thermal and thermo-oxidative behaviour of the different kinds of polyethylene. Figures 4 and 5 show the thermogravimetric curves obtained in nitrogen and in air, respectively; the characteristic degradation temperatures are summarized in Table 4.

In inert atmosphere, the degradation of either LDPEs or HDPEs samples occurs in a single degradation step. As observable from the data listed in Table 4, the thermal degradation of HDPEs, irrespective of the viscosity of the samples, starts at 425 °C and ends at about 500 °C. At variance, for LDPEs, the temperatures involved are slightly lower, with degradation starting in the range 390-405 °C. The differences noticed between the investigated materials can be related to the different structure of the PEs and, in particular, to their different content of tertiary carbon. In fact, the lower thermal stability of both LDPE samples can be correlated to their higher content of tertiary carbon as compared to HDPEs [25]. Also, the slight differences observed between LDPE_LV and LDPE_HV can be ascribed to the different macromolecular architecture of the two samples in terms of different branching degree and, hence, to the different content of tertiary carbon [26].

The TGA curves obtained in an oxidative atmosphere show a different degradation behaviour. In fact, the thermal oxidative degradation of either LDPEs or HDPEs samples takes place in a complex process, induced by the destabilization effect of the oxygen that reacts with the degrading polymer radicals during the heating. In particular, the thermal oxidative mechanism involves two main steps

of weight loss [27-28]. Besides, a third minor step can be noticed at higher temperatures; this last can be attributed to the oxidation of the charred residue formed by the oxidative dehydrogenation of the polymers occurring during the heating process in oxidative atmosphere [15]. As compared to the thermal degradation in inert atmosphere, the oxidative degradation of all studied materials starts at lower temperatures (280-298 °C), with some remarkable differences among the different samples, which could be ascribed to the different structure and architecture of the polymer chains and to their possible influence on the interactions between oxygen and the degrading radicals during the polymer degradation, as well as between the radicals themselves.

Table 4. Main results from TGA in nitrogen and air for all investigated samples.

	Nitrogen		Air		
Material	**$T_{2\%}$ [°C]**	**T_{max} [°C]**	**$T_{2\%}$ [°C]**	**T_{max1} [°C]**	**T_{max2} [°C]**
HDPE_LV	425	481	296	403	457
HDPE_HV	425	484	280	413	443
LDPE_LV	392	474	280	376	418
LDPE_HV	406	478	298	397	420

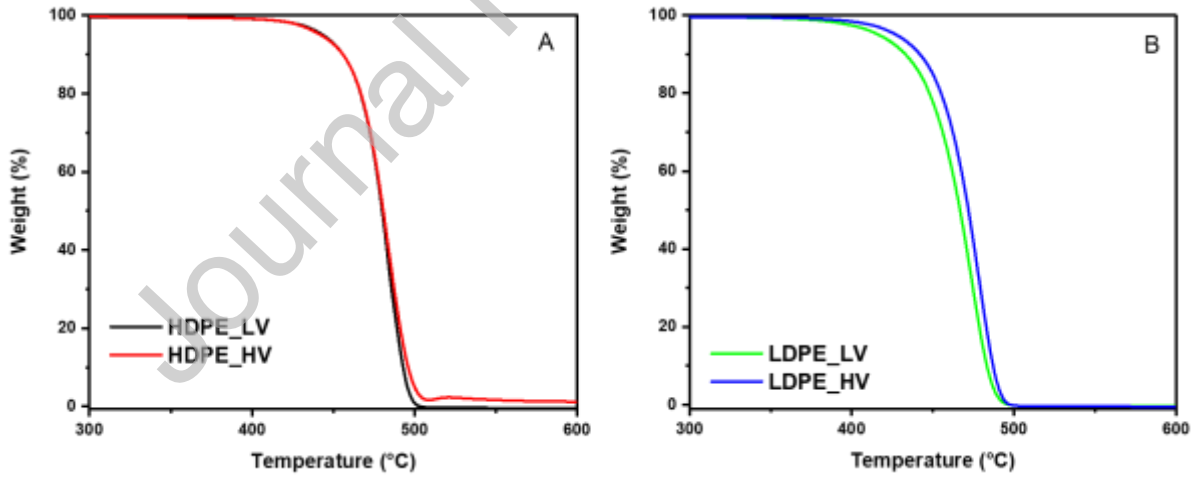

Figure 4. TG curves for HDPEs (A) and LDPEs (B) samples in nitrogen.

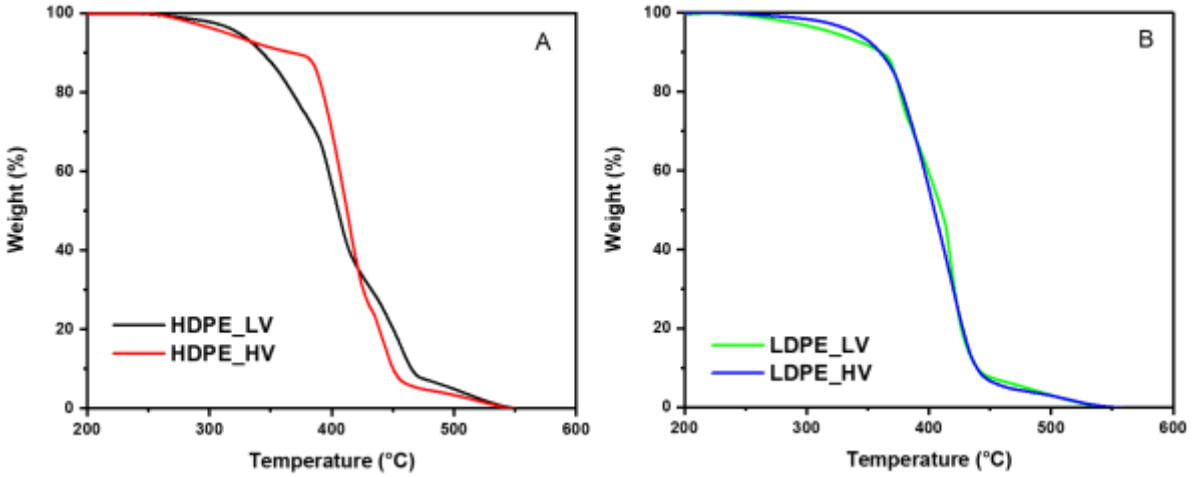

Figure 5. TG curves for HDPEs (A) and LDPEs (B) samples in air.

3.2 Char formation

3.2.1 Isothermal-dynamic heating

The results of TGA performed in oxidative atmosphere have highlighted different behaviours between the samples, in terms of both thermo-oxidative stability and degradation temperatures. In order to better understand the phenomena occurring during the heating in the presence of oxygen, isothermal-dynamic thermo-gravimetric analyses were performed. The samples were first heated in air at 320 °C (i.e., just 20-40 °C above the weight loss onset of all samples), and held at that temperature for 60 min; then, the samples were heated to 650 °C with a heating rate of 10 °C/min. Figures 6 A-B show the results obtained for HDPEs and LDPEs samples, respectively. Regardless of the different macromolecular architecture and viscosity, all the investigated materials are prone to form a residue during the isothermal step, due to the well-known ability of polyethylene to form char in isothermal conditions under an oxidative atmosphere [15].

However, significant differences arise when comparing the trends and the values of the residues obtained for the different samples. In particular, HDPE_HV shows a modest weight loss at the beginning of the isothermal step, followed by a plateau that indicates the formation of a stable black residue. The behaviour of HDPE_LV is very similar to that of HDPE_HV, although in this case a more pronounced weight loss is observed when the isothermal step starts, resulting in a lower residue. At the end of the isothermal treatment, the obtained residues are 79 and 68 % (see the values reported in Table 5) for HDPE_HV and HDPE_LV, respectively. It is interesting to highlight that the residues of both materials, when dynamic heating is switched on, are stable up to 380 °C, i.e., about 100 °C higher than the original HDPEs,; then, they rapidly volatilise leaving a 10% char at 450 °C, which is finally completely oxidised to volatiles at 550 °C as in dynamic TGA in air (Figure 5A).

Looking at the trends of the LDPEs samples, it can be observed that LDPE_LV shows a behaviour quite similar to that of HDPEs; in fact, after a weight loss in the first 10 to 15 minutes, the formation of a stable residue is achieved, with a residue at the end of the isothermal step of 77%. However, differently to what was observed for HDPEs samples, in this case, the residue is no longer stable when the dynamic heating is applied, and the weight starts to decrease immediately at the end of the isothermal step. The behaviour of LDPE_HV is completely different as, in this case, a continuous decrease of the weight during the isothermal step can be observed. Actually, the drop of the weight as a function of time has not a monotonic trend, but it seems to follow a sort of multi-step tendency (as observable from the derivative – dTG – curves reported in Figure S1), meaning that the material could be able to form a residue that, however, is not stable over the time. Irrespectively of the different behaviour exhibited by the sample during the isothermal step, the formed residues rapidly volatilise upon dynamic heating, producing about 20% char at 450 °C, which is fully oxidised at 550 °C, again as in dynamic TGA (Figure 5B).

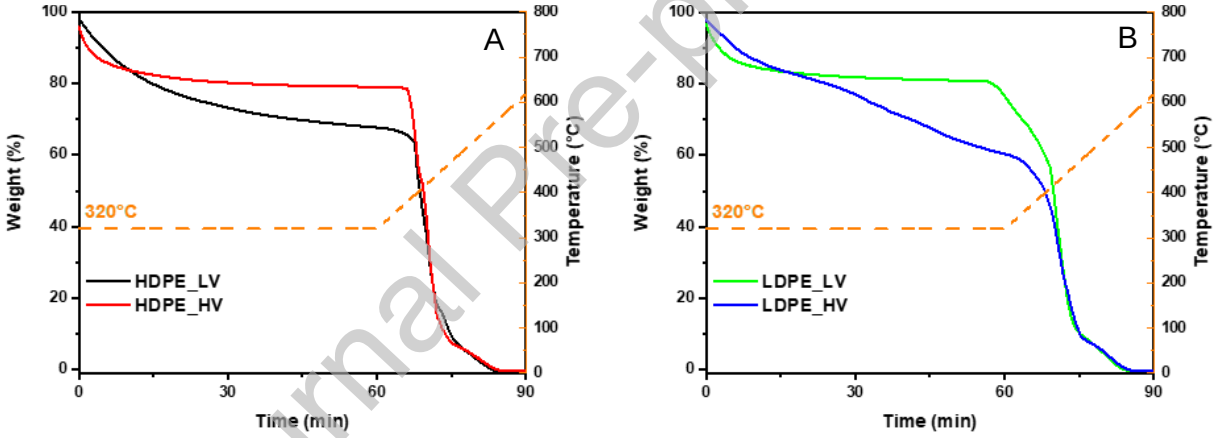

Figure 6. Isothermal TG curves for 60 min at 320°C, then heated to 650°C (10°C/min) for HDPEs (A) and LDPEs (B) samples.

Table 5. Residual weight of the HDPEs and LDPEs samples after the isothermal step at 320 °C.

Material	Residual weight after isothermal (%)
HDPE_LV	68
HDPE_HV	79
LDPE_LV	77
LDPE_HV	60

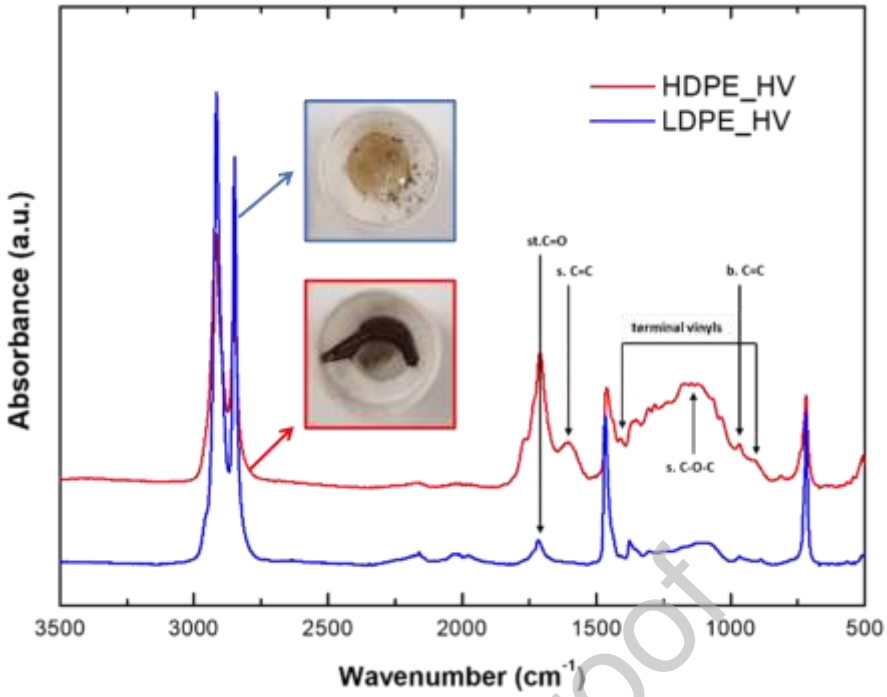

Figure 7. ATR-FTIR spectra for HDPE_HV and LDPE_HV samples after the isothermal-dynamic TGA and pictures of the residues collected at the end of the isothermal step.

In order to deeply inspect the different behaviour shown by the samples during the isothermal-dynamic heating, the residues recovered at the end of the isothermal step were collected and characterized. In particular, the analysis was focused on HDPE_HV and LDPE_HV samples, representing the two materials exhibiting completely opposite behaviour. Figure 7 reports the ATR-FTIR spectra collected on the materials after the heating treatment, along with the pictures of the two residues. Significant differences can be observed already from a qualitative examination of the collected residues. In fact, it can be clearly noticed that HDPE_HV forms a black-coloured residue, which can be ascribed to the formation of double bonds and aromatic rings typical of the charring phenomenon. At variance, in the case of LDPE_HV, just some yellowing/browning of the material can be observed. The analysis of the collected spectra confirms what is inferred from the visual inspections of the residues. In particular, the spectrum of LDPE_HV shows the appearance of a band centred at 1718 cm^{-1} that can be attributed to the formation of carbonyl groups resulting from the thermal oxidation undergone by the sample during the heating treatment. Besides, two weak absorption peaks at 1410 and 908 cm^{-1}, associable with the formation of terminal vinyl groups deriving from the chain-scission of the polymer backbone [29], appear. HDPE_HV sample, apart from the already described signals (which are more intense as compared to LDPE_HV) exhibits further signals, namely: an intense and broad absorption band in the range 1160-1130 cm^{-1}, which can be related to the formation of aliphatic esters (C-O-C stretching), and two broad peaks at 1604

and 968 cm^{-1}, likely due to C=C aromatic stretching and C=C bending, respectively [30]. These last peaks confirm the occurrence of cross-linking and charring phenomena during the thermal treatment, at least on the surface of HDPE_HV samples. The gathered results about the different structure of the residues obtained for the two materials can be thus related to the different behaviour shown during the isothermal-dynamic TGA. More specifically, it is possible inferring that the formation of an aromatic structure at least on the surface of HDPE_HV is responsible for the stable behaviour exhibited by the material during the isothermal treatment (see Figure 6A). Conversely, the continuous weight decrease during the isothermal step observed for LDPE_HV (Figure 6B) can be explained by considering the continuous degradation of the sample during the entire test.

3.3 Pre-ignition behaviour

The chemical/physical modifications occurring in the PEs pre-ignition step were studied on the samples exposed to 20 or 35 kW/m^2 in the Cone Calorimeter.

The surface temperature increase of the four materials, from the beginning of exposure to ignition is shown in Figure 8. In all cases, the heating rate shows a transition from a higher to a lower rate linear regime located around the melting temperature, corresponding to the transition from the higher thermal capacity of the melt compared to the solid. This shows that the ignition and combustion of PE is the ignition and combustion of a liquid, in spite of the original solid feature of the PE material.

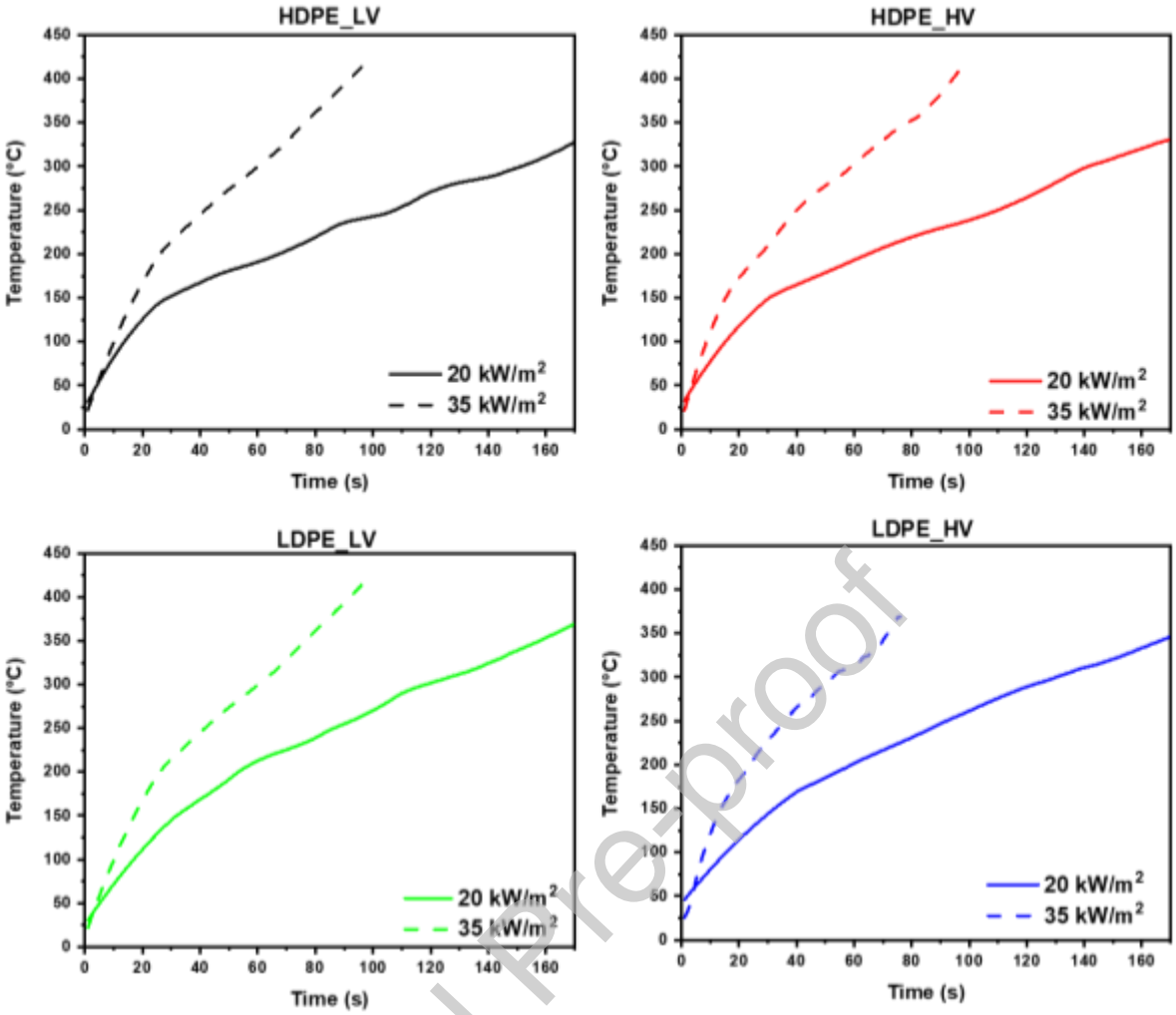

Figure 8. temperature profiles of HDPE and LDPE specimens at 20 and 35 kW/m^2.

Typically, in the pre-ignition step, the PEs exposed at 20 or 35 kW/m^2 are heated at a rate ranging from around 100 to 200 °C/min. It is observed that surface discolouration progressively develops from yellow to brown and black colour on heating, as shown in Figure 9 for samples quenched at ignition time.

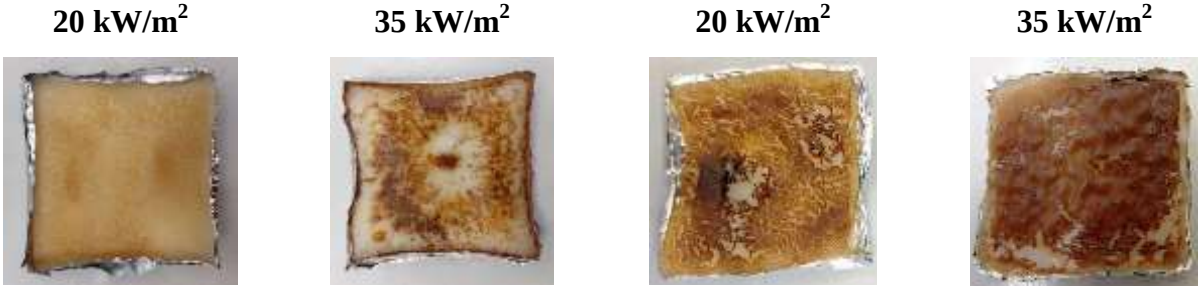

LDPE_LV **LDPE_HV**

Figure 9. Appearance of the surface of specimens quenched at ignition time during cone calorimeter tests at 20 and 35 kW/m^2.

The data concerning the four PEs are summarised in Table 6: in spite of their very similar chemical structure, the samples behave significantly differently in the pre-ignition step.

Table 6. Times and temperatures recorded at a heat flux of 20 and 35 kW/m^2.

Material	Starting char formation time (s)	Starting char formation temperature (°C)	Time to Ignition (s)	Temperature at Ignition (°C)
Heat flux of 20 kW/m^2				
HDPE_LV	130	287	173	332
HDPE_HV	150	311	240	435
LDPE_LV	140	316	178	383
LDPE_HV	120	289	178	353
Heat flux of 35 kW/m^2				
HDPE_LV	80	363	100	426
HDPE_HV	70	334	97	416
LDPE_LV	80	340	90	407
LDPE_HV	70	342	80	378

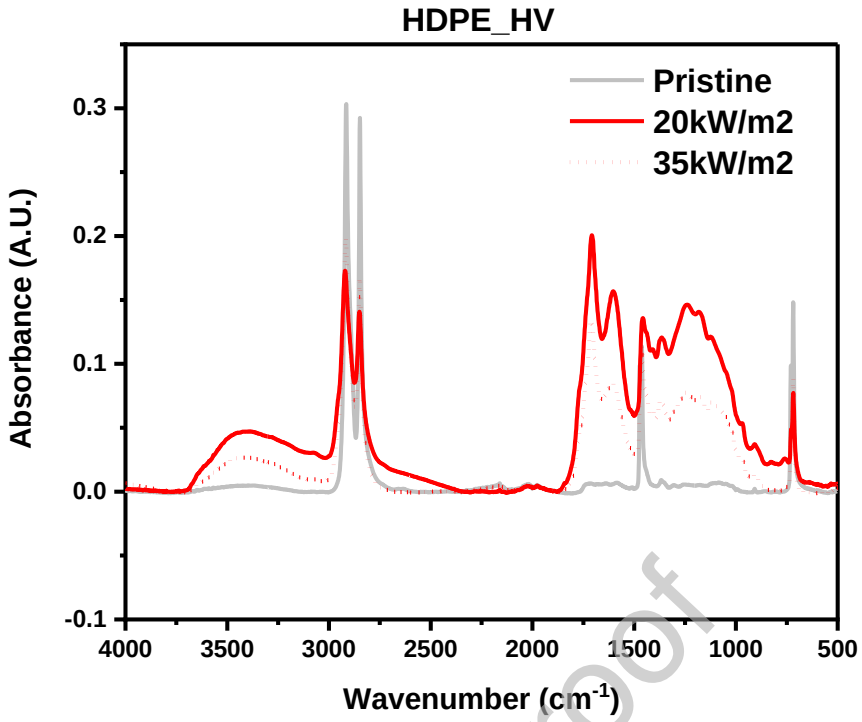

Figure 10. ATR spectra of the pristine HDPE_HV surface specimen, and after irradiation in the cone calorimeter at heat fluxes of 20 and 35 kW/m^2.

The surface chemical modifications induced by heat exposure in the cone calorimeter are shown in Figure 10 by the ATR-FTIR spectrum taken from a sample of HDPE_LV at ignition time. An extensive modification of the original PE polyhydrocarbon structure is confirmed by the strong decrease in the intensity of the absorptions due to the original C-H bonds at 2915, 2848, 1472, 1463, 728 and 719 cm^{-1} and the build-up of strong absorptions at 3000-3700, 1710, 1606, 800-1500 cm^{-1} respectively, corresponding to OH, C=O, C=C, C-O chemical bonds. All these features indicate that a dehydrogenation-oxidative process has taken place by the reaction of oxygen of air with the molten PE.

Figure 10 shows that the level of chemical modification of the PE surface when ignition conditions are reached decreases when irradiance increases. This is due to the kinetic control typical of heterophasic gas-condensed phase chemical reactions, owing to the rate control by the gas diffusion into the condensed phase. With irradiance increase in the cone calorimeter, the sample heating rate increases with the decrease of oxygen solubility and oxygen diffusion rate into the molten PE. This induces a decrease of the bimolecular oxygen-PE reaction rate compared to lower irradiance so that, when the temperature, at which ignition occurs, is reached, lower surface chemical modifications result compared to lower irradiance.

Similar results are obtained with the LDPE_HV and LDPE_LV (Figure S2) whereas HDPE_LV exhibits a lower concentration of surface oxidised groups at ignition time, as shown by the broad absorption band at 800-1500 cm^{-1} (Figure S2).

4. Discussion

The obtained results showed that, despite the very similar chemical structure of the studied polymers, they show different behaviour in isothermal-dynamic heating conditions and during the pre-ignition step, as far as the char formation mechanism is concerned. Therefore, in the following, the observed dissimilar behaviour will be explained considering two different approaches, namely a chemical and a microstructural approach. More specifically, the mechanism of char formation will be discussed referring to the influence of the effect of the chemical structure of the samples (part 4.1) and of the different macromolecular architecture and topology (part 4.2).

4.1 Discussion Part 1: chemical approach

4.1.1 The ignition scenario

Piloted or auto-ignition of a polymer material exposed to a heat source occurs when above its surface, the local concentration of the volatile products issued by the polymer degradation, reaches their lower flammability limit or the auto-ignition conditions respectively. The instantaneous transient volatiles concentration above the material surface depends on the competition between the flux of the volatile products from the degrading material and their diffusion flux in the environment. The balance between the two fluxes for a given material, in a defined fluid dynamic regime, primarily depends on the temperature reached by the material, which controls the rate of its thermal volatilization. Hence, the time required to reach the ignition conditions depends on the heating rate of the irradiated material, which results from the thermal flux from the heat source and controls the time evolution of the material's temperature [31].

Apart from its physical environmental surrounding, the ignition behaviour of a polymer material exposed to a heating source also depends on its chemical reactivity toward oxygen of air. Polymers that react with dioxygen on heating, may undergo volatilization at a lower temperature in air than in inert atmosphere or under vacuum. In such cases, polymer ignition would depend on the flammability of the volatile products of thermal oxidation of the polymer rather than on the products issued from the thermal scission of the polymer chemical bonds.

4.1.2 PEs thermal and thermo-oxidative degradation mechanisms

Polyhydrocarbons such as PE are typical examples of oxygen-sensitive polymers, whose thermal volatilization occurs at a lower temperature when heated in air than in inert atmosphere [32-33]. In nitrogen, the thermal volatilization of the HDPEs takes place around 420 °C (Table 4), through a radical chain mechanism initiated by random homolytic C-C bond scission of the PE macromolecular chain, whose dissociation energy (ca. 85 kcal/mol) is lower than that of the other chemical bonds of PE (ca. 100 kcal/mol for C-H). The result is the quantitative volatilisation of PE to a complex mixture of saturated and unsaturated hydrocarbons [34].

The LDPEs chain branching makes their thermal degradation in nitrogen initiate at a temperature about 20-30 degrees lower than that of HDPEs (Table 4). This is due to the (CH_3)C-C bond of the branching tertiary carbon, which is characterized by a bond dissociation energy (80 kcal/mole) lower than that of the secondary C-C bonds of the PE chains.

In air, HDPEs and LDPEs start losing weight at a temperature about 135 and 110°C lower than in nitrogen, respectively (Table 4), due to the occurrence of oxidative dehydrogenation reaction [32]. Three quite distinct temperature regimes before the TTI of PEs, each characterized by a quite different chemistry, have been recognized. The first is the "low" temperature regime (T ~< 160°C), the second is the so-called "cool" flame region (between 250-400 °C), and the third is the region of hot ignition, above 450-500 °C [35]. The PEs throughout the ignition time are within the cool flame region (as shown in Figure 8). Therefore, the polymers in the cone calorimeter before ignition will decompose by two involved mechanisms, partially overlapping: hydroperoxidation and dehydrogenation [35].

Unlike hydroperoxidation that leads to oxidised functional groups on the PEs chain, dehydrogenation favours the formation of polyunsaturated PEs (as shown by ATR-FTIR of Figure 7), which tend to develop into conjugated polyenes owing to the increased mobility of the allylic hydrogens of dehydrogenated PE (dissociation energy for allylic C-H: 85 kcal/mol) which promotes a “zipper” type of reaction [36].

The conjugated unsaturations explain the discolouration reaching the black colour observed during PEs pre-ignition. In fact, sequences of more than five to seven conjugated unsaturated bonds absorb within the visible light spectral range with wavelength absorption upshift when the polyene length increases [36]. From Figure 7 (inset) and Figure 10 compared with S2, it can be seen that these reactions, leading to the black colouration of the residue and a significant absorbance of the FTIR band in the region between 1500 and 800 cm^{-1}, are more significant in HDPE_HV sample than in the others. This result can be explained by the greater stability of the material, which is more resistant to thermal oxidation (see Table 4) and thus delays the volatilisation of the degraded chain pieces by promoting the formation of stable residues.

4.1.3 PEs charring

Crosslinking accompanying the PEs thermal oxidation increases the C-C dissociation temperature. In fact, the mobility of the macromolecular radical fragments issued by C-C scission of the crosslinked PEs, necessary to reach a permanent bond scission by their diffusion, is hindered by the rigidity of the crosslinked structure. Several C-C bonds must be contemporarily dissociated, which are close enough to produce relatively small mobile radical polymer fragments that would otherwise recombine instead of diffusing apart. To increase the probability of this statistically controlled event, the temperature should be raised in order to increase the total number of bonds dissociating simultaneously. Volatilisation is however hindered by competition with allylic hydrogen abstraction of the dehydrogenating crosslinked PEs, which provides them with a polyunsaturated crosslinked aromatic, polyaromatic-like structure. The resulting thermally stable residue is a carbon-rich black material called “char” [37].

The crosslinked char structure is responsible for the weight loss trends observed in Figure 6, where the stabilization of the PEs heated in air at 320 °C, which is in dehydrogenation conditions, is provided by the surface build-up of the char layer that may hinder the oxygen access to the polymer. When the temperature is increased, the thermal stability of the char structure built at 320°C is overcome and weight loss resumes to total volatilization. A difference in behaviour between HDPE_HV and HDPE_LV can be seen in terms of the amount of stable residue. In fact, LDPEs, as soon as the temperature starts to rise again, lose weight (see Figure 6). This means that the formed structures do not have the same stability. From the chemical point of view of the structures, this difference should be negligible; therefore, the observed phenomena could be likely related to the different macromolecular architecture of the investigated samples, as deeply discussed below.

4.1.4 Degradation mechanisms in PEs pre-ignition

During the exposure to 20kW/m^2 in the cone calorimeter, within the first 40 s, the PEs undergo oxidation essentially by hydroperoxidation, when the samples surface temperature reaches about 150 °C while PEs melting is occurring to completion.

Conversely, after 100 s when the sample reaches 250 °C, oxidative dehydrogenation essentially occurs, with evidence of surface discolouration/charring beginning at about 120 s (sample temperature: 300 °C), proceeding then to dark black colour till ignition at 180 s (sample at 330-380 °C). In the range of 40-100 s, oxidation in the “cool flame” regime takes place, in which hydroperoxidation and dehydrogenation are likely to overlap.

On dynamic heating, volatiles are issued by thermal oxidation of PEs beginning at about 300 °C (Table 4), which are reached by the surface exposed to the cone calorimeter in 120 s. In this range of temperatures, oxidative dehydrogenation begins producing volatiles by allylic bond scission of conjugated polyenes that are likely to be the flammable polymer fragmentation products that ignite. Exposure to 35 kWm^2 shortens the time to ignition as it could be expected because the sample surface temperature increases more rapidly than at 20 kW/m^2 (see Figure 8). The degradation reactions rate increases, increasing the flux of the flammable volatiles contrasting environment diffusion so that the lower flammability limit concentration is reached earlier. Nonetheless, the range of temperatures of the sample surface in the pre-ignition time is the same at both heat fluxes. In particular, oxidative dehydrogenation is the source of ignited volatiles in both cases.

4.2 Discussion Part 2: microstructural approach

Since the rheological characterization demonstrated that the samples are characterized by a different macromolecular architecture, this latter may have some influence on the mechanisms and kinetics of char formation. In particular, as described above, the mechanism of char formation in polyethylene proceeds through oxidative dehydrogenation reactions resulting in conjugated polyenes, which further undergo cross-linking, until the formation of char [37]. Therefore, the kinetics of the charring mechanism and the stability of the formed char are strongly affected by the promptness of the polymer macromolecules in interacting with the surrounding chains to form crosslinked structures, representing the precursors of the carbonaceous residue. Aiming at verifying the possible different tendency of the chains of the different PE samples in establishing polymer-polymer interactions when subjected at high-temperature treatments, time sweep tests were performed on all the investigated materials.

The obtained results are depicted in Figure 11, in terms of variation of the storage modulus (G') as a function of time. Since G' is related to the elastic component of the polymer viscoelastic behaviour, an increase of this property as a function of time indicates the occurrence of phenomena, such as cross-linking or melt structuring, inducing an amplification of the elastic characteristics of the material. As observable in Figure 11, all the investigated materials exhibit a continuous increase of G' for the whole duration of the test, with some remarkable differences that are discussed in the following. In particular, HDPE_HV shows a more rapid rise of the storage modulus as compared to the other samples, suggesting that its macromolecules possess a high propensity to interact in a very easy and fast way. This result could be associated with the high molecular weight of HDPE_HV, resulting in a highly entangled structure. Furthermore, the linear topology of the HDPE_HV chains allows for close proximity between adjacent macromolecules, further promoting the establishment

of a great number of chain-chain interactions, possibly resulting in the formation of crosslinking that induces the growth of G'. The great tendency of interaction and the high level of proximity of the HDPE_HV macromolecules can be related to the high charring ability of this material, since the high the extent of stable interaction between neighbouring chains, the high the feasibility in forming a char with a durable structure.

Differently, the rate of increase of the storage modulus of HDPE_LV is significantly lower as compared to HDPE_HV. In fact, the values of the slope of the curves depicted in Figure 11 (evaluated in the final part of the test), associable with a sort of build-up rate of G', are 13.6 and 6.5 for HDPE_HV and HDPE_LV, respectively. This result is likely due to the low molecular weight of this sample that, resulting in a poorly entangled and compact structure, does not allow for a rapid activation of the interaction modes between adjacent macromolecules, thus hindering the achievement of a high degree of cross-linking. The lower promptness of the HDPE_LV macromolecules in interacting with the surrounding chains has an influence on the charring ability of this material, since the slow kinetics of chain interaction reflects in the formation of a lower amount of char with respect to HDPE_HV (see values in Table 5). Furthermore, as observed in Figure 6A, during the isothermal step the char formation rate is lower for HDPE_LV as compared to HDPE_HV.

The behaviour of LDPE_LV is quite similar to that of the HDPE_LV, in terms of both charring ability and increase of G', notwithstanding the lower value of the build-up rate (slope value: 4.1). In fact, although this sample presents a branched structure, its main rheological features (i.e., low viscosity values, Newtonian behaviour, liquid-like relaxation) seem to suggest that the architecture of the LDPE_LV chains is almost linear, characterized by the presence of a low degree of short-chain branching. Therefore, also in this case, the material is able to form char, since the presence of short-chain branching does not compromise the establishment of effective chain/chain interactions.

LDPE_HV shows a growth of G' as a function of time, which is quite similar to that of LDPE_LV sample (slope value for LDPE_HV: 4.6). Nevertheless, the macromolecular architecture of the two materials is significantly different, since the microstructure of LDPE_HV (as assessed by the rheological measurements) is characterized by the presence of a great number of long-chain branching points. Actually, in the case of LDPE_HV, it should be taken into account that different chain/chain, branch/branch, chain/branch and/or intra-branch interactions are established when the sample is heated at high temperature. Although one can imagine the formation of a highly entangled structure, it is possible inferring that, as entanglements are formed mainly between the long-chain branches, the establishment of effective and stable interactions leading to the formation of cross-linking is more difficult as compared to linear polymers. As reported in the literature, the presence

of long-chain branches influences the formation of effective entanglement networks, thereby affecting the crosslinking efficiency, as polymeric chains with high contents of long-chain branching are more prone to disentangle [38]. Besides, as demonstrated by Smedberg et al. [39-40], the coils formed by long-chain branched polymers usually have smaller dimensions as compared to the more extended coils typical of linear macromolecular structures, and this issue causes the achievement of intramolecular crosslinks (i.e., within its own coil), while hampering crosslinks with adjacent polymer coils, thus leading to a lower crosslinking efficiency than linear polymers.

On the other hand, the non-monotonic weight decrease as a function of time obtained during the isothermal TG measurements (see Figure 6B) corroborates this hypothesis, since it seems that LDPE_HV has a certain tendency in forming char, but the formed char is not stable when the material is maintained at high temperature, thus resulting in a progressive degradation also in isothermal conditions.

The effect of the different macromolecular architecture of the studied PEs samples is less noticeable in the behaviour shown during the cone calorimetry tests. As a matter of fact, also in this case it can be recognized a higher ability of HDPE_HV in promoting char formation with respect to other samples, which can be ascribed to the highest rate of interaction between its long linear macromolecules, resulting in the achievement of a highly entangled and compact structure. Nevertheless, the very rapid heating of the sample surface when subjected to heat fluxes of 20 kW/m^2 or, even more, at 35 kW/m^2 causes a minimization of the differences between the various samples (as clearly observed in Figure 9). As discussed before, this finding is due to the extremely high kinetic of the involved degradation reactions, which induces a progressive anticipation of the time to ignition.

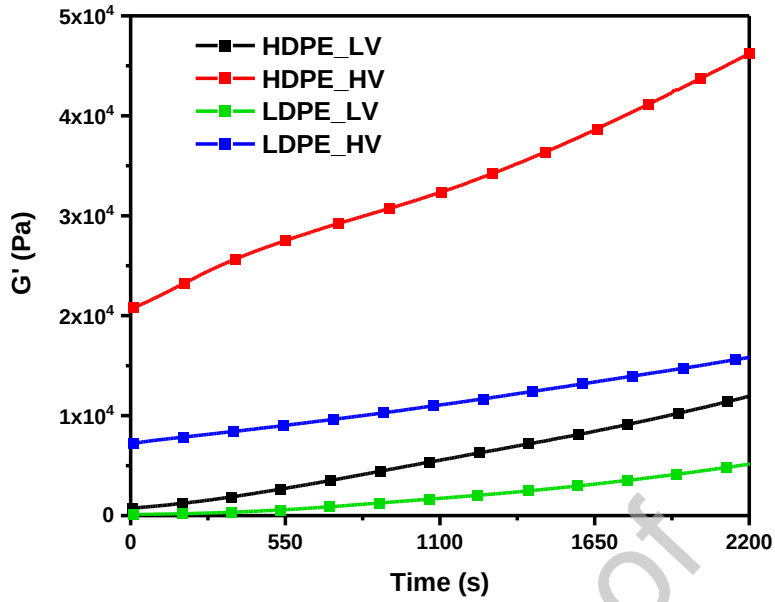

Figure 11. Storage modulus (G') as a function of time for all investigated materials.

4.Conclusions

In this work, the charring ability of four different samples of polyethylene was thoroughly evaluated. Two HDPE samples characterized by different molecular weights and two LDPE materials, differing in the branching structure, were selected, aiming at disclosing the possible relationships between the polymer macromolecular architecture and the mechanism and kinetics of char formation. After a preliminary characterization of the samples, which allowed for assessing their different microstructure, isothermal thermogravimetric analyses were carried out. The obtained results demonstrated a different charring ability of the investigated samples, also confirmed through cone calorimetry tests performed by subjecting the materials to different heat fluxes. The observed behaviours were then discussed taking into consideration the different chemical structure of the materials: this approach revealed some differences in the mechanisms of degradation and char formation between high-density and low-density PEs. Furthermore, as outlined by rheological analyses, the different charring ability of the materials was related to the intrinsic tendency of the macromolecules of the selected PEs in interacting in the molten state. In particular, it has been demonstrated that the linear chain structure of HDPE (especially in the case of high molecular weight polymers) leads to the establishment of strong interactions between the macromolecules (due to their close proximity), enabling the formation of a well-developed crosslinking network, which is likely able to further evolve into a stable char. Conversely, the presence of long-chain

branched structures increases the distance between the polymer backbones, making more difficult the establishment of strong and durable interactions, notwithstanding the formation of a highly entangled structure. This issue might compromise the formation of a stable char for long-chain branched LDPE, which, indeed, showed a lower charring ability. The observed behaviors were minimized when the surface of the samples was rapidly heated during the cone calorimetry tests at heat fluxes of 20 kW/m^2 or, even more, of 35 kW/m^2, likely due to the progressive anticipation of the time to ignition resulting from the remarkably high kinetic of the involved degradation reactions.

In all, the obtained results could be very useful in increasing the knowledge on the PE's charring ability, allowing for predicting its intrinsic tendency in char formation, which represents a fundamental stage of its fire behaviour, and in selecting the more appropriate flame-retardant strategy depending on the polymer macromolecular architecture and on the specific fire scenario.

Acknowledgements

The authors want to thanks Mr. Samuele Matta for the preparation of samples and cone tests.

CRediT author statement

Alberto Frache: Conceptualization, Methodology, Writing - Review & Editing **Rossella Arrigo:** Methodology, Investigation, Writing – Original Draft **Giulio Malucelli:** Writing - Review & Editing **Giovanni Camino**: Conceptualization, Writing - Original Draft

References

[1] Morgan, A.B.; Gilman, J.W. An overview of flame retardancy of polymeric materials: application, technology, and future directions. Fire and Materials 2013, 37, 259-279.

[2] Fina, A.; Camino G. Ignition mechanisms in polymer and polymer nanocomposite. Polymers for Advanced Technologies 2011, 22, 1147-1155.

[3] Malucelli, G.; Carosio, F.; Alongi, J.; Fina, A.; Frache, A.; Camino, G. Materials engineering for surface-confined flame retardancy. Materials Science and Engineering: R: Reports 2014, 84, 1-20.

[4] Price, D.; Anthony, G.; Carty, P. Introduction: polymer combustion, condensed phase pyrolysis and smoke formation. In: Fire Retardant Materials. Editors: Horrocks, A.R.; Price, D. Woodhead Publishing 2001, 1-30.

[5] Fina, A.; Feng, J.; Cuttica, F. In-depth radiative heat transmittance through polypropylene/nanoclay composites. Polymer Degradation and Stability 2013, 98, 1030-1035.

[6] Martel, B. Charring processes in Thermoplastic Polymers: Effect of Condensed Phase Oxidation on the Formation of Chars in Pure Polymers. Journal of Applied polymer Science 1988, 35, 1213-1226.

[7] Stoliarov, S.I.; Crowley, S.; Lyon, R.E.; Linteris, G.T. Prediction of the burning rates of non-charring polymers. Combustion and Flame 2009, 156, 1068-1083.

[8] Luche, J.; Mathis, E.; Rogaume, T.; Richard, F.; Guillaume, E. High-density polyethylene thermal degradation and gaseous compound evolution in a cone calorimeter. Fire Safety Journal 2012, 54, 24-35.

[9] Lewin, M.; Weil, E.D. Mechanisms and modes of action in flame retardancy of polymers. In: Fire Retardant Materials. Editors: Horrocks, A.R.; Price, D. Woodhead Publishing 2001, 31-68.

[10] Pal, G.; Macskasy, H. Plastics: Their behavior in fires. Elsevier, New York, 1991.

[11] Laoutid, F.; Bonnaud, L.; Alexandre, M.; Lopez-Cuesta, J.M.; Dubois, Ph. New prospects in flame retardant polymer materials: From fundamentals to nanocomposites. Materials Science and Engineering R 2009, 63, 100-125.

[12] Babrauskas, V. Development of the cone calorimeter – A bench-scale heat release rate apparatus based on oxygen consumption. Fire and Materials 1984, 8, 81-95.

[13] Hirschler, M.M. Flame retardants and heat release: review of data on individual polymers. Fire and Materials 2015, 39, 232–258.

[14] Karlsson, B.; Quintiere, J.G. A Qualitative Description of Enclosure Fires in Enclosure Fire Dynamics, CRC Press LLC, New York, 1999.

[15] Costantino, U.; Montanari, M.; Nocchetti, M.; Canepa, F.; Frache, A. Preparation and characterisation of hydrotalcite/carboxyadamantane intercalation compounds as fillers of polymeric nanocomposites. Journal of Materials Chemistry 2007, 17, 1079-1086.

[16] Ran, S.; Zhao, L.; Han, L.; Guo,Z.; Fang, Z. Improvement of the thermal and thermo-oxidative stability of high-density polyethylene by free radical trapping of rare earth compound. Thermochimica Acta 2015, 612, 55-62.

[17] Mirabella, F.M.; A. Bafna. Determination of the crystallinity of polyethylene/α-olefin copolymers by thermal analysis: Relationship of the heat of fusion of 100% polyethylene crystal and the density. Journal of Polymer Science Part B: Polymer Physics 2002, 40, 1637-1643.

[18] Honerkamp, J.; Weese, J. A nonlinear regularization method for the calculation of relaxation spectra. Rheologica Acta 1993, 32, 65-73.

[19] Gulmine, J.V.; Janissek, P.R. Heise, H.M.; Akcelrud, L. Polyethylene characterization by FTIR. Polymer Testing 2002, 21, 557-563.

[20] Munaro, M.; Akcelrud, L. Correlations between composition and crystallinity of LDPE/HDPE blends. Journal of Polymer Research 2008, 15, 83-88.

[21] Fu, Q.; Men, Y.; Strobl, G. Understanding of the tensile deformation in HDPE/LDPE blends based on their crystal structure and phase morphology. Polymer 2003, 44, 1927-1933.

[22] Peacock, A. Handbook of Polyethylene Structures: Properties, and Applications. Marcel Dekker, Inc. 2000.

[23] Chen, C.; Shekh, M.I.; Cui, S.; Stadler, F.J. Rheological Behavior of Blends of Metallocene Catalyzed Long-Chain Branched Polyethylenes. Part I: Shear Rheological and Thermorheological Behavior. Polymers 2021, 13, 328.

[24] Stadler, F.J.; Arikan-Conley, B.; Kaschta, J.; Kaminsky, W.; Münstedt, H. Synthesis and Characterization of Novel Ethylene-graft-Ethylene/Propylene Copolymers. Macromolecules 2011, 44, 5053-5063.

[25] Abbas-Abadi, M.S. The effect of process and structural parameters on the stability, thermo-mechanical and thermal degradation of polymers with hydrocarbon skeleton containing PE, PP, PS, PVC, NR, PBR and SBR. Journal of Thermal Analysis and Calorimetry 2021, 143, 2867-2882.

[26] Luyt, A.S.; Malik, S.S.; Gasmi, S.A.; Porfyris, A.; Andronopoulou, A.; Korres, D.; Vouyiouka, S.; Grosshauser, M.; Pfaendner, R.; Brüll, R.; Papaspyrides, C. Halogen-Free Flame-Retardant Compounds. Thermal Decomposition and Flammability Behavior for Alternative Polyethylene Grades. Polymers 2019, 11, 1479.

[27] Bocchini, S.; Frache, A.; Camino, G.; Claes, M. Polyethylene thermal oxidative stabilisation in carbon nanotube based nanocomposites. European Polymer Journal 2007, 43, 3222-3235.

[28] Zhao, L.; Guo, Z.; Cao, Z.; Zhang, T.; Fang, Z.; Peng, M. Thermal and thermo-oxidative degradation of high density polyethylene/fullerene composites. Polymer Degradation and Stability 2013, 98, 1953-1962.

[29] Zanetti, M.; Bracco, P.; Costa, L. Thermal degradation behaviour of PE/clay nanocomposites. Polymer Degradation and Stability 2004, 85, 657-665.

[30] Allen, N.S.; Edge, M.; Rodriguez, M.; Liauw, C.M.; Fontan, E. Aspects of the thermal oxidation of ethylene vinyl acetate copolymer. Polymer Degradation and Stability 2000, 68, 363-371.

[31] Irvine, D.J.; McCluskey, J.A.; Robinson, I.M. Fire hazards and some common polymers. Polymer Degradation and Stability 2000, 67, 383-396.

[32] Al-Malaika, S. Effects of anti-oxidants and stabilizers. In: Comprehensive Polymer Science. Editors: Allen, G.; Bevington, J.C. Pergamon 1989, 539-578.

[33] Halley, P.J.; Graeme, G.A. Chemorheology of Polymers - From Fundamental Principles to Reactive Processing. Cambridge University Press, United Kingdom, 2009.

[34] Costa, L.; Camino, G. Thermal degradation of polymer-fire retardant mixtures: Part V. Polyethylene-chloroparaffin mixtures. Polymer Degradation and Stability 1985, 12, 105-116.

[35] Benson, S.W. The kinetics and thermochemistry of chemical oxidation with application to combustion and flames. Progress in Energy and Combustion Science 1981, 7, 125-134.

[36] Holmstrom, A.; Sorvik, E. Thermal degradation of polyethylene in a nitrogen atmosphere of low oxygen content. II. Structural changes occuring in low-density polyethylene at an oxygen content less than 0.0005%. Journal of Appled Polymer Science 1974, 18, 761-778.

[37] Lomakin, S.M.; Novokshonova, L.A.; Brevnov, P.N.; Shchegolikhin, A.N. Thermal properties of polyethylene/montmorillonite nanocomposites prepared by intercalative polymerization. Journal of Materials Science 2008, 43, 1340-1353.

[38] Andersson, L.H.U.; Hjertberg, T. The effect of different structure parameters on the crosslinking behaviour and network performance of LDPE. Polymer 2006, 47, 200-210.

[39] Smedberg, A.; Hjertberg, T.; Gustafsson, B. Effect of molecular structure and topology on network formation in peroxide crosslinked polyethylene. Polymer 2003, 44, 3395-3405.

[40] Smedberg, A.; Hjertberg, T.; Gustafsson, B. The role of entanglements in network formation in unsaturated low density polyethylene. Polymer 2004, 45, 4867-4875.

CRediT author statement

Alberto Frache: Conceptualization, Methodology, Writing - Review & Editing **Rossella Arrigo:** Methodology, Investigation, Writing – Original Draft **Giulio Malucelli:** Writing - Review & Editing **Giovanni Camino**: Conceptualization, Writing - Original Draft

Declaration of interests

☒The authors declare that they have no known competing financial interests or personal relationships that could have appeared to influence the work reported in this paper.

☐The authors declare the following financial interests/personal relationships which may be considered as potential competing interests: